



ELSEVIER

<http://dx.doi.org/10.1016/j.ultrasmedbio.2017.01.001>

● Original Contribution

EVALUATION OF CORONARY ARTERY DISEASE USING MYOCARDIAL ELASTOGRAPHY WITH DIVERGING WAVE IMAGING: VALIDATION AGAINST MYOCARDIAL PERFUSION IMAGING AND CORONARY ANGIOGRAPHY

JULIEN GRONDIN,* MARC WAASE,[†] ALOK GAMBHIR,^{†1} ETHAN BUNTING,* VINCENT SAYSING,*
 and ELISA E. KONOFAGOU*[‡]

*Department of Biomedical Engineering, Columbia University, New York, New York, USA; [†]Department of Medicine, Columbia University, New York, New York, USA; and [‡]Department of Radiology, Columbia University, New York, New York, USA

(Received 3 November 2016; revised 19 December 2016; in final form 4 January 2017)

Abstract—Myocardial elastography (ME) is an ultrasound-based technique that can image 2-D myocardial strains. The objectives of this study were to illustrate that 2-D myocardial strains can be imaged with diverging wave imaging and differ, on average, between normal and coronary artery disease (CAD) patients. In this study, 66 patients with symptoms of CAD were imaged with myocardial elastography before a nuclear stress test or an invasive coronary angiography. Radial cumulative strains were estimated in all patients. The end-systolic radial strain in the total cross section of the myocardium was significantly higher in normal patients ($17.9 \pm 8.7\%$) than in patients with reversible perfusion defect ($6.2 \pm 9.3\%$, $p < 0.001$) and patients with significant ($-0.9 \pm 7.4\%$, $p < 0.001$) and non-significant ($3.7 \pm 5.7\%$, $p < 0.01$) lesions. End-systolic radial strain in the left anterior descending, left circumflex and right coronary artery territory was found to be significantly higher in normal patients than in CAD patients. These preliminary findings indicate that end-systolic radial strain measured with ME is higher on average in healthy persons than in CAD patients and that ME has the potential to be used for non-invasive, radiation-free early detection of CAD. (E-mail: Ek2191@columbia.edu) © 2017 World Federation for Ultrasound in Medicine & Biology.

Key Words: Cardiac strain imaging, Diverging wave imaging, Coronary artery disease, Myocardial perfusion imaging, Coronary angiography.

INTRODUCTION

Coronary artery disease (CAD) is characterized by an insufficient blood flow in the coronary arteries and can lead to heart attack and myocardial infarct. It is the leading cause of death worldwide, with 8.1 million deaths in 2013 (Roth et al. 2015), and accounted for approximately 1 of every 7 deaths in the United States in 2011 (Mozaffarian et al. 2015). Various methods are used to diagnose ischemia, such as electrocardiogram (ECG) stress testing, stress echocardiography and nuclear stress tests, or to assess coronary anatomy using coronary

computed tomography angiography or magnetic resonance coronary angiography (Montalescot et al. 2013). Stress echocardiography is an ultrasound technique and therefore has the advantages of portability, low risk and of high temporal resolution. However, it requires the myocardium to be stressed either by exercising or pharmacologically and is based mainly on a visual assessment of wall motion abnormalities, which is subjective. Studies have focused on left ventricular systolic function, as it has been reported to be a strong predictor of long-term survival in patients affected by various cardiac diseases (Sveav et al. 2008; Vasan et al. 1999).

Echocardiographic strain imaging has been developed as an ultrasound-based method to objectively and quantitatively assess myocardial deformation during stress or at rest (Gaibazzi et al. 2014; Zuo et al. 2015). Strain imaging offers the advantage of distinguishing tissue motion with deformation from tissue motion without significant deformation, and several studies

Address correspondence to: Elisa E. Konofagou, Department of Biomedical Engineering, 1210 Amsterdam Avenue, ET 351, MC 8904, New York, NY 10027, USA. E-mail: Ek2191@columbia.edu

Conflict of interest disclosure: The authors declare no conflicts of interest.

¹Present address: Northeast Georgia Heart Center, Gainesville, GA, USA.

have reported that strain and strain rate imaging are sensitive to myocardial damage after myocardial ischemia or infarction (Edvardsen et al. 2001; Voigt et al. 2003; Weidemann et al. 2007; Winter et al. 2007). The two commercially available cardiac strain imaging techniques are tissue Doppler imaging (TDI) (Hoffmann et al. 2010; Urheim et al. 2000) and speckle tracking echocardiography (STE) (Biering-Sorensen et al. 2014; Gaibazzi et al. 2014). However, TDI is angle-dependent and has low spatial resolution, and STE is performed with B-mode images, which are based on the envelope of the radiofrequency (RF) signals. Previous studies have indicated that the RF signals provide better performance than envelope signals for tissue deformation estimation (Alam and Ophir 1997; Ma and Varghese 2013). Myocardial elastography (ME) is an angle-independent technique for 2-D myocardial strain imaging at high temporal resolution using RF signals (Zervantonakis et al. 2007). This technique has been validated against tagged magnetic resonance imaging and was found to be able to differentiate normal from reperfused myocardium (Lee et al. 2008). A more recent study indicated that ME is capable of detecting, identifying and characterizing down to 40% blood flow reduction in the left anterior descending artery (LAD) of a canine model *in vivo* (Lee et al. 2011). In these previous studies, high frame rates were achieved while maintaining a high beam density by using ECG gating to assemble small sectors of RF signals acquired at different heartbeats into a full echocardiographic view. Not only can this composite sector data acquisition cause mismatches between sectors that can lead to motion artifacts, but also requires the patients to hold their breath during the 20-s duration of acquisition to minimize motion artifacts, which can be challenging for diseased patients.

In this study, the performance of ME by acquiring RF signals at high frame rates during a single heart cycle was investigated. To acquire the full echocardiographic view during a single heart cycle at high frame rate, diverging wave imaging was used. Previous studies have reported that diverging wave imaging can be used to image the heart with high contrast at high temporal resolution (Papadacci et al. 2014) or follow the propagation of the electromechanical wave in the heart at high temporal resolution by estimating inter-frame strains (Provost et al. 2013) and was validated against electrical mapping (Grondin et al. 2016). Diverging wave imaging has also been used to image cardiac end-systolic cumulative axial strains in patients with an intracardiac transducer to differentiate healthy tissue from RF lesion (Grondin et al. 2015). The feasibility and precision of estimating axial and lateral cardiac strain using diverging wave imaging has also been illustrated in healthy volunteers,

but without accumulating the strain over systole (Bunting et al. 2014). However, the use of diverging wave imaging for investigating normal and CAD patients by comparing end-systolic accumulated cardiac strain has not yet been investigated.

The objectives of this study were to illustrate that 2-D myocardial strains can be imaged in normal and CAD patients with diverging wave imaging and to investigate the difference in end-systolic radial strains measured between normal and CAD patients.

METHODS

Study population

In this study, the end-systolic radial strain estimated with ME was compared with two widely used techniques to diagnose CAD. Patients with symptoms of CAD and scheduled for a nuclear stress test or an invasive coronary angiography were screened. Patients with prior known myocardial infarct, stent, bypass surgery, heart transplants, severe aortic stenosis, hypertrophic heart, weight >220 pounds or a poor acoustic window were excluded from the study. All patients who did not have those exclusion criteria and who gave their informed consent were recruited. Of the 66 patients recruited for this study, 17 were assessed by coronary angiography and 49 were assessed by nuclear perfusion imaging. The study protocol was approved by an institutional review board of Columbia University, and informed consent was obtained before the study.

Myocardial elastography

The patients were scanned at rest with ultrasound before and on the same day as their nuclear stress test or angiography. None of the patients were sedated before the ultrasound scan. The heart was imaged in short-axis view at the basal, mid- and apical levels. A 2.5-MHz center frequency transducer (P4-2, ATL/Philips, Andover, MA, USA) operated by a Verasonics system (V-1, Verasonics, Kirkland, WA, USA) was used to scan the patients. The ECG signal was acquired synchronously with the ultrasound data using an ECG unit (77804 A, HP, Palo Alto, CA, USA) connected to a data acquisition system (NI USB-6210, National Instruments, Austin, TX, USA) and triggered by the Verasonics system. To obtain a large field of view at high frame rate (2000 Hz), diverging wave imaging was used by placing the focus 10 mm behind the surface of the transducer (Provost et al. 2011, 2013). Channel RF data were acquired at 2000 Hz on the 64 elements of the probe during 2 s and sampled at 10 MHz. A standard delay-and-sum method was used to reconstruct the entire image for each single diverging beam transmit (Grondin et al. 2015). The image was reconstructed on a polar grid of 256 lines, sampled

axially at 20 MHz (*i.e.*, $38.5 \mu\text{m}$) with an imaging depth of 20 cm and a field of view of 90° . Conventional B-mode images were also acquired during 1.5 s. Motion estimation was performed at 500 Hz using normalized 1-D (axial) cross-correlation (Luo and Konofagou 2010) in a 2-D (axial and lateral) search (Konofagou and Ophir 1998) with a window length of 5.9 mm and 90% overlap. The lateral search range was 1 beam with a 10:1 linear interpolation factor. A 3×3 -mm median filter was applied to the axial and lateral displacements to reduce outliers associated with peak-hopping artifacts. The axial and lateral displacements were accumulated during systole, which is commonly defined using ECG landmarks such as the RT interval (Budoff and Shinbane 2010). However, as illustrated in Figure 1, the axial displacement M-mode exhibits some transient motion between the R peak and the onset of the inward motion, consistently observed in all patients. Because this transient motion can affect the displacement accumulation, systole was defined from the axial displacement M-mode during the inward motion. More specifically, the onset of systole was manually selected and defined as the beginning of the longest phase during which the anterior wall exhibited a downward motion (in *blue*) while the inferior wall concomitantly exhibited an upward motion (in *red*).

The myocardium was manually segmented and automatically tracked (Luo and Konofagou 2008) throughout the systolic phase. Axial and lateral Lagrangian strains were estimated from the axial and lateral displacements, respectively, using a least-squares estimator implemented with Savitzky–Golay filters (Luo *et al.* 2004). Radial strains were derived from the axial and lateral strains with the origin of the polar coordinate system at the centroid of the segmented myocar-

dium. Previous studies had found that end-systolic radial strain was able to differentiate a reperfused from a normal myocardium (Lee *et al.* 2008) and to characterize early onset of ischemia (Lee *et al.* 2011). In this study, for each patient, the end-systolic radial strain was averaged in the entire cross section of the myocardium in the short-axis view. The reproducibility of this technique was investigated in a healthy subject and in two CAD patients. The end-systolic radial strain was compared between two acquisitions from consecutive cardiac cycles or after removal and repositioning of the probe. Radial strains were obtained from ultrasound acquisition in short-axis view, which is more convenient for assessing the distribution of each main coronary artery.

Territory selection

The myocardium was divided into three major coronary vascular territories as defined by the general assumption about the most frequent vascular distribution pattern as illustrated in Lauerma *et al.* (1997). Each of the three regions of interest (ROIs) was manually selected from the B-mode image. The LAD perfuses the anteroseptal region, the left circumflex artery (LCX) perfuses the lateral region and the right coronary artery (RCA) perfuses the inferior region. The end-systolic radial strain was averaged in each of the three territories.

Myocardial perfusion imaging

At rest, the patient was injected with $^{99\text{m}}\text{Tc}$ sestamibi, and rest gated perfusion images of the heart were obtained using a dual-head Philips Precedence SPECT/CT camera (Philips Healthcare, Amsterdam, Netherlands) equipped with low-energy, high-resolution collimators. Each patient was stressed *via* Bruce treadmill exercise protocol if capable of ambulating or *via* a pharmacologic vasodilator agent (regadenoson or adenosine, depending on physician preference). At peak stress, patients were injected with $^{99\text{m}}\text{Tc}$ sestamibi and again imaged with a SPECT/CT camera. The tomographic slices were reconstructed in three orthogonal planes (short axis, horizontal long axis and vertical long axis). The reconstructed images were analyzed using both visual and quantitative analysis. All images were assessed by a nuclear cardiology board-certified physician.

Coronary angiography

The patients were brought to the procedure room and placed on the table. Left and right coronary angiography was performed by advancing a catheter to the aorta and positioning it in the ostium of the left main coronary artery and the right coronary, respectively. Angiography was performed in multiple projections. Omnipaque (GE Healthcare, Chicago, IL, USA) was used as a

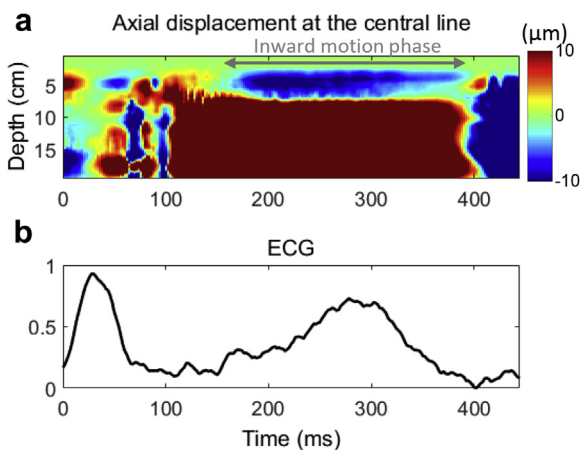


Fig. 1. Axial displacement M-mode (a) and corresponding electrocardiogram (ECG) (b). Negative displacements in *blue* indicate downward motion, and positive displacements in *red* indicate upward motion.

contrast agent. All images were assessed by a cardiology board-certified physician. Patients with >50% obstruction in a coronary vessel on the angiogram were considered to have significant CAD, whereas patients with ≤50% obstruction were considered to have non-significant CAD.

Statistical analysis

All statistical analyses were performed using MATLAB (The MathWorks, Natick, MA, USA). A χ^2 -test was used to investigate if the distribution of categorical variables in Table 1 differed. The mean and standard deviation of end-systolic mean radial strain across patients were computed for the normal patients, the patients with reversible myocardial perfusion defect (group 1), the patients with non-significant CAD and the patients with significant CAD (group 2) for the total cross-section of the myocardium as well as for each ROI. A Lilliefors test was used to determine if the end-systolic mean radial strain for every group of patients in each territory and in the total cross section followed a normal distribution. The end-systolic mean radial strains in the normal group and in group 1 were normally distributed in each territory and in the total cross section, and a two-sample *t*-test was used to compare each quantity. A one-way analysis of variance (ANOVA) test for normally distributed quantities and a Kruskal–Wallis test for non-normally distributed quantities were performed to compare the end-systolic mean radial strain between the normal, non-significant CAD and significant CAD patients. For the normal patients, the end-systolic mean radial strain was computed at the mid-level short-axis view, whereas for the CAD patients it was computed at the level (apical, middle or basal) with abnormal perfusion. If several levels had abnormal perfusion for a given CAD patient, the mid-level was

used because of higher strain estimation quality at this level.

RESULTS

Among the recruited patients, 36 were normal (34 patients with normal myocardial perfusion assessed by nuclear stress test and 2 patients with normal coronary arteries determined by angiography), 15 had myocardial ischemia detected by nuclear perfusion (group 1) and 15 had coronary stenosis determined by angiography (group 2). The patient population is described in Table 1. Of the patients who underwent coronary angiography, 6 were found to have non-significant CAD, whereas 9 were found to have significant CAD. Six patients were found to have single-vessel CAD, 2 patients were found to have double-vessel CAD and 7 patients were found to have triple-vessel CAD (significant and/or non-significant). The numbers of patients with significant and non-significant CAD for each coronary artery are detailed in Table 1.

Strain imaging

All healthy patients and CAD patients were in sinus rhythm during ultrasound data acquisition. The reproducibility of ME with diverging wave imaging was investigated in a normal patient, a CAD patient from group 1 and a CAD patient from group 2. Left-ventricular, end-systolic radial strains in the total cross-section were found to be $26.1 \pm 31.5\%$ versus $25.1 \pm 38.3\%$ for two consecutive cardiac cycles in a normal patient (Fig. 2); $6.1 \pm 15.9\%$ versus $10.8 \pm 17.7\%$ after removal and repositioning of the probe in a patient with a reversible perfusion defect in the inferior wall (Fig. 3a, 3b); $0.6 \pm 11.8\%$ versus $0.1 \pm 7.0\%$ for two consecutive cardiac cycles in a patient with 50% occlusion in the ostium of the first diagonal of the LAD (Fig. 3c, 3d). Similar

Table 1. Clinical characteristics of the 66 patients*

| | Normals (n = 36, 54.6%) | CAD group 1 (n = 15, 22.7%) | CAD group 2 (n = 15, 22.7%) | p value | |
|------------------------|----------------------------|--------------------------------|--------------------------------|----------------------------|----------------------------|
| | | | | Normals vs. CAD group 1 | Normals vs. CAD group 2 |
| Age (y) | 61.2 ± 11.2 | 68.0 ± 9.7 | 59.3 ± 12.9 | 0.064 | 0.510 |
| Males | 15 (41.7%) | 10 (66.7%) | 11 (73.3%) | 0.104 | 0.039 |
| Hypertension | 20 (55.6%) | 10 (66.7%) | 11 (73.3%) | 0.463 | 0.236 |
| Diabetes | 13 (36.1%) | 0 (0%) | 1 (6.7%) | 0.007 | 0.032 |
| Smoker | 11 (30.1%) | 4 (26.7%) | 9 (60.0%) | 0.781 | 0.050 |
| Chronic kidney disease | 4 (11.1%) | 2 (13.3%) | 0 (0%) | 0.822 | 0.179 |
| Pulmonary disease | 0 (0%) | 1 (6.7%) | 1 (6.7%) | 0.118 | 0.118 |
| Coronary disease | | | >50% | | ≤50% |
| LAD | 0 | 4 | 7 | | 8 |
| LCX | 0 | 8 | 5 | | 10 |
| RCA | 0 | 9 | 5 | | 10 |

CAD = coronary artery disease; LAD = left anterior descending artery; LCX = left circumflex; RCA = right coronary artery.

* Groups 1 and 2 comprise patients with CAD detected by nuclear stress test and coronary angiography, respectively.

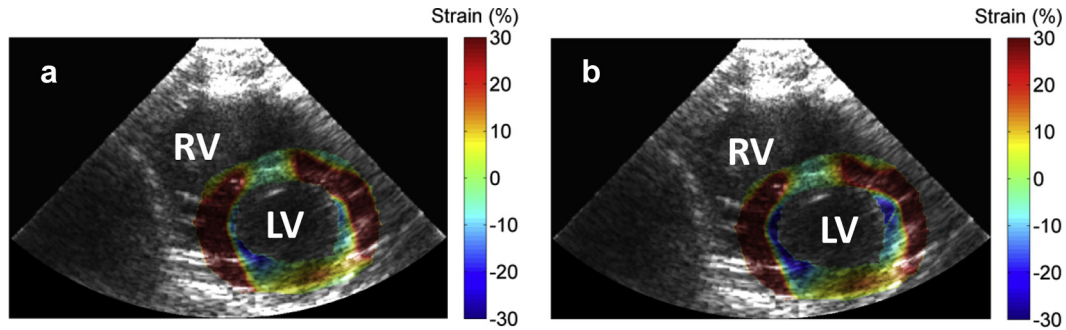


Fig. 2. Left ventricular, end-systolic radial strain for two consecutive cardiac cycles (a,b) in a normal individual. A similar pattern was obtained for both acquisitions, which indicates the good reproducibility of the technique. LV = left ventricle; RV = right ventricle.

patterns were obtained for both acquisitions for the normal and CAD patients. Left-ventricular, end-systolic radial strain in a normal subject is illustrated in [Figure 2](#). Positive radial strains in *red* reveal radial thickening of the myocardium. Myocardial elastography was also performed in CAD patients. Left-ventricular, end-systolic radial strain is seen in a patient with a reversible perfusion defect in the inferior wall ([Fig. 3a, 3b](#)). Radial thickening (in *red*) was measured in the anterior and septal regions, whereas radial thinning (in *blue*) was measured in the inferior and lateral regions. Left ventricular, end-systolic radial strain is seen in a patient with 50% occlusion in the ostium of the first diagonal of the

LAD ([Fig. 3c, 3d](#)). Radial thickening was measured in the anterior, lateral and inferior regions, whereas radial thinning was measured in the septal region.

Statistical analysis

The myocardium was divided into three territories, each of which was perfused by a coronary artery ([Lauerma et al. 1997](#)). The mean and standard deviation of end-systolic radial strain were computed in the total cross section of the myocardium as well as in each territory for the normal patients and compared with those obtained in group 1 of the patients with CAD detected by nuclear perfusion imaging ([Fig. 4](#)) and group 2 of

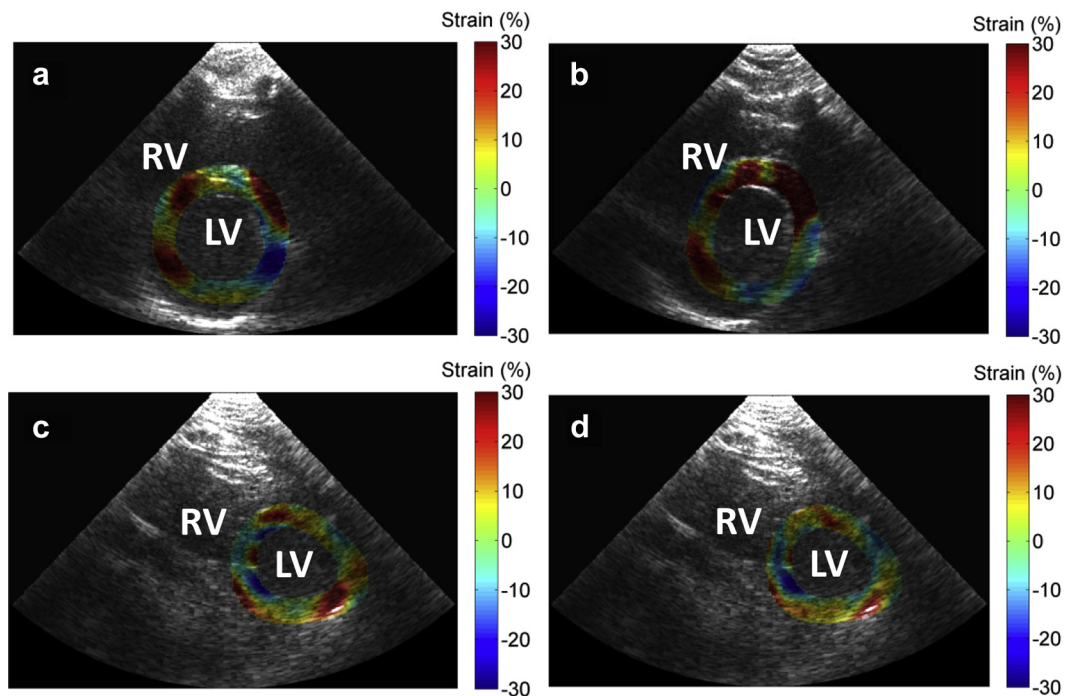


Fig. 3. Left-ventricular, end-systolic radial strains in a patient with a reversible perfusion defect in the inferior wall for two acquisitions after repositioning of the probe (a,b) and in a patient with 50% occlusion in the ostium of the first diagonal of the left anterior descending artery for two consecutive cardiac cycles (c,d). LV = left ventricle; RV = right ventricle.

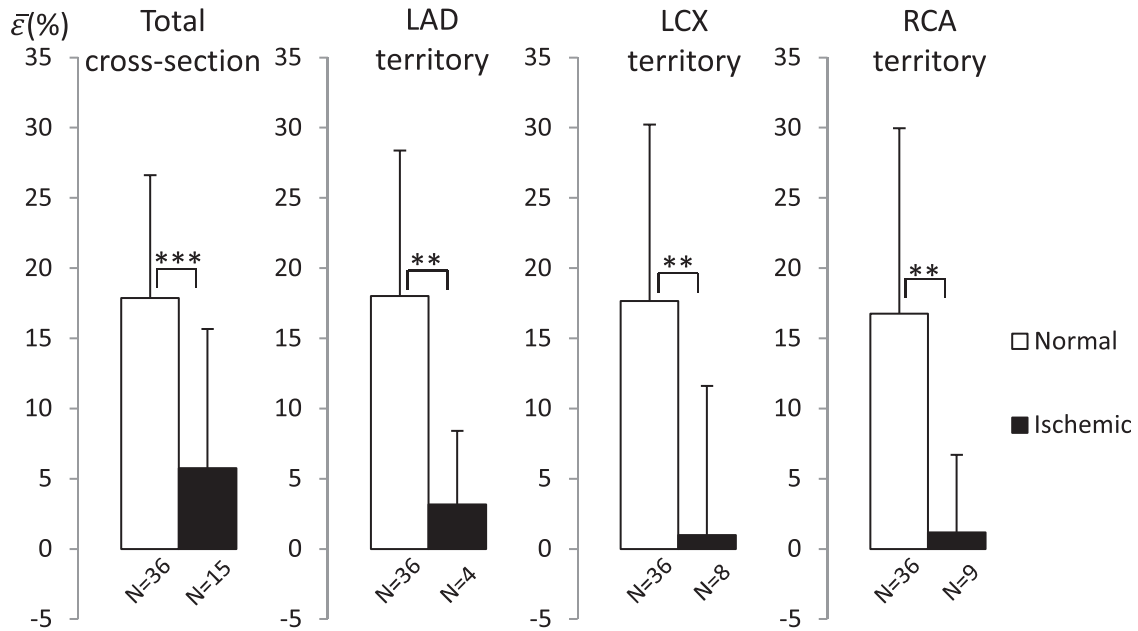


Fig. 4. Left ventricular, end-systolic mean radial strain ($\bar{\epsilon}$) in normal and ischemic (group 1) patients in the total cross section of the myocardium and left anterior descending artery (LAD), left circumflex artery (LCX) and right coronary artery (RCA) territory. Error bars indicate standard deviations across the patients. $**p < 0.01$; $***p < 0.001$.

the patients with CAD detected by coronary angiography (Fig. 5). The end-systolic radial strain in the total cross-section of the myocardium in healthy patients ($17.9 \pm 8.7\%$) was significantly higher than that in the group 1 CAD patients ($6.2 \pm 9.3\%$, $p < 0.001$). End-systolic

radial strain in the LAD territory was found to be significantly higher in healthy patients ($18.0 \pm 10.4\%$) than in patients with perfusion defect in regions perfused by the LAD ($3.2 \pm 5.2\%$, $p < 0.01$). End-systolic radial strain in the LCX territory was found to be significantly higher in

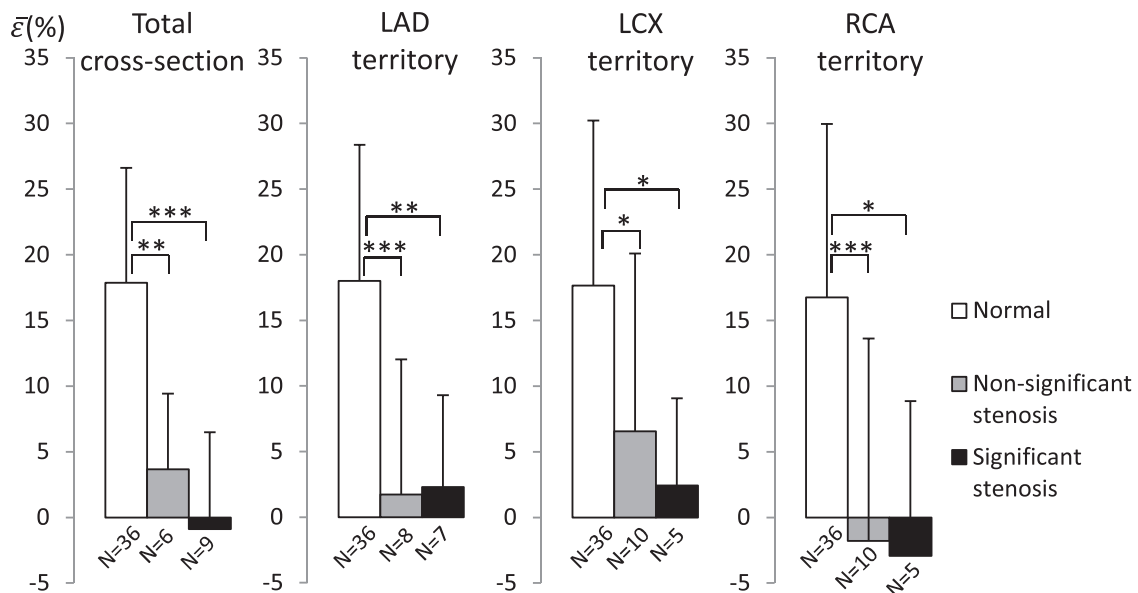


Fig. 5. Left ventricular, end-systolic mean radial strain ($\bar{\epsilon}$) in normal, non-significant CAD and significant coronary artery disease patients (group 2) in the total cross section of the myocardium and left anterior descending (LAD), left circumflex artery (LCX) and right coronary artery (RCA) territory. Error bars indicate standard deviations across the patients. $*p < 0.05$; $**p < 0.01$; $***p < 0.001$.

healthy patients ($17.7 \pm 12.6\%$) than in patients with perfusion defect in regions perfused by the LCX ($1.0 \pm 10.6\%$, $p < 0.01$). End-systolic radial strain in the RCA territory was found to be significantly higher in healthy patients ($16.8 \pm 13.2\%$) than in patients with perfusion defect in regions perfused by the RCA ($1.2 \pm 5.5\%$, $p < 0.01$).

The end-systolic radial strain in the total cross-section of the myocardium in healthy patients ($17.9 \pm 8.7\%$) was significantly higher than that in patients with significant CAD ($-0.9 \pm 7.4\%$, $p < 0.001$) and patients with non-significant CAD ($3.7 \pm 5.7\%$, $p < 0.01$). End-systolic radial strain in the LAD territory was found to be significantly higher in healthy patients ($18.0 \pm 10.4\%$) than in patients with obstructed LAD ($2.3 \pm 7.0\%$, $p < 0.01$) and patients with non-significant LAD ($1.7 \pm 10.3\%$, $p < 0.001$). End-systolic radial strain in the LCX territory was found to be significantly higher in healthy patients ($17.7 \pm 12.6\%$) than in patients with obstructed LCX ($2.4 \pm 6.6\%$, $p < 0.05$) and patients with non-significant LCX ($6.6 \pm 13.5\%$, $p < 0.05$). The end-systolic radial strain in the RCA territory was found to be significantly higher in healthy patients ($16.8 \pm 13.2\%$) than in patients with obstructed RCA ($-2.9 \pm 11.8\%$, $p < 0.05$) and patients with non-significant RCA ($-1.8 \pm 15.4\%$, $p < 0.001$). No significant difference was found between patients with non-significant CAD and those with significant CAD in the total cross section of the myocardium or in any territory.

DISCUSSION

Non-invasive and non-ionizing detection and characterization of CAD can avoid unnecessary procedures and radiation exposure such as coronary angiography and nuclear stress tests. It has been reported that only 35% to 40% of patients referred for a nuclear stress test have at least one reversible defect (Hoiland-Carlsen *et al.* 2006; Shaw *et al.* 1999), indicative of ischemia, and 53% to 62% of patients referred for a coronary angiography turn out to have normal or non-significant CAD (Hoiland-Carlsen *et al.* 2006; Patel *et al.* 2010). ME is an echocardiography-based technique that can image myocardial strains at high frame rate using the RF signals. High-frame-rate imaging can be achieved using sector scan acquisition of focused beams and ECG gating. This technique requires long breath-holding times to reduce motion artifacts and uses acquisition from multiple cardiac cycles. ME has been found capable of differentiating a normal heart from a reperfused heart or a heart with reduced blood flow in the LAD using ECG-gated acquisitions. Our objectives were to illustrate that 2-D myocardial strain can be imaged in normal and CAD patients during a single heart cycle at high temporal resolu-

tion and to investigate the difference in end-systolic radial strain between normal and CAD patients.

The reproducibility of our technique was investigated for normal and CAD patients. Left-ventricular, end-systolic radial strains were obtained for each patient during two consecutive cardiac cycles or after removing and repositioning the probe. Similar radial strains were obtained for both acquisitions for the normal and CAD patients, with better reproducibility of ME with diverging waves for consecutive cardiac cycles than after removal and repositioning of the probe. Figure 2 illustrates the left-ventricular, end-systolic radial strains in a normal subject. Radial thickening of the myocardium is observed in the entire cross-section. This indicates that ME with diverging wave imaging can be used to image 2-D myocardial strains transthoracically during a single heart cycle.

Left-ventricular, end-systolic radial strains were also imaged for CAD patients. Figure 3a and b illustrates radial strain for a patient with a reversible perfusion defect in the inferior wall, indicative of ischemia. The anterior and septal regions indicate radial thickening, whereas the inferior and lateral regions indicate thinning. This region of opposite strain can be the result of passive tethering caused by the ischemia. This effect has been reported in previous studies (Holmes *et al.* 2005), predicted by theoretical models (Lee *et al.* 2007) and imaged by ME and tagged MRI (Lee *et al.* 2008). Figure 3c and d illustrate radial strain for a patient with 50% occlusion in the ostium of the first diagonal of the LAD. Radial thickening is observed in the anterior, lateral and inferior regions, whereas thinning is observed in the septal wall, which is perfused by the LAD.

Figure 4 compares the left ventricular, end-systolic radial strain in normal and ischemic patients across the entire cross section of the myocardium as well as in the LAD, LCX and RCA territories. Ischemic patients were found to have significantly lower radial strains than normal patients across the total cross section of the myocardium, as well as in the LAD, LCX and RCA territories. This suggests that ME can distinguish normal from CAD patients. Figure 5 compares the left-ventricular, end-systolic radial strain in normal, non-significant CAD and significant CAD patients across the entire cross-section of the myocardium, as well as in the LAD, LCX and RCA territories. Patients with non-significant and significant CAD were found to have significantly lower radial strains than normal patients across the total cross section of the myocardium as well as in the LAD, LCX and RCA territories. Previous studies reported that non-significant lesions can cause ischemia (Curzen *et al.* 2014; Park *et al.* 2015; Schuijff *et al.* 2006). However, in this study, no significant difference in radial strain was observed between patients with

non-significant CAD and patients with at least one obstructed coronary in the total cross section or in any territory. The significant difference between normal and ischemic patients or patients with non-significant CAD indicates that ME could be used for early detection of CAD. However, the level of stenosis was visually assessed. Therefore the classification between significant and non-significant coronary stenosis can be affected by the subjectivity of the operator. In addition, among the 15 patients found with stenosis, 12 were reported to have had a clinical echocardiogram independently of this study and only 5 of the 12 were found to have wall motion abnormality. Among the 7 patients reported with normal wall motion, 4 had non-significant occlusions and 3 had significant occlusions. This indicates that the ultrasound-based technique presented in this study can measure lower strain in patients with coronary stenosis compared with healthy patients whereas wall motion scoring assessed by clinical echocardiography was not sensitive enough to coronary stenosis in most of the patients. In this study, 36 patients were normal, 15 had reversible perfusion defect and 15 had significant or non-significant stenosis. A larger-scale study should be carried out to determine if these preliminary findings are confirmed in the total cross section of the myocardium, as well as in the LAD, LCX and RCA territories. A larger number of patients would also be required to investigate the effect of the severity of the stenosis on the strain measurements.

This study has several limitations. The groups of CAD patients and normal patients had a few clinical characteristic differences that could have an effect on heart function. The proportions of males and of smokers were significantly higher among the group 2 CAD patients than among the normal patients. On the other hand, the proportion of patients with diabetes was significantly higher in the normal group than in both groups of CAD patients.

As mentioned previously, diverging wave imaging was used in this study to image the heart during a single heartbeat and at a relatively high frame rate to minimize decorrelation of RF signals. Therefore, the transmit waves were not focused and produced a lower lateral resolution compared with focused waves, which can impair the lateral motion estimation. Lateral and radial strain estimation can thus be affected. However, our preliminary results suggest that the left ventricular end-systolic radial strains differ significantly between normal and CAD patients. Because the acquisition and motion estimation frame rates were 2000 and 500 Hz, respectively, coherent compounding of diverging waves can be used to increase the lateral resolution while maintaining a relatively high frame rate and still imaging within a single

heart cycle. This technique is currently under investigation to be used with ME.

The division of the entire cross section of the myocardium into the LAD, LCX and RCA territories, although based on anatomic landmarks, was performed manually. This can affect the strain values attributed to each territory. An automated method would remove the subjectivity in the territory division. However, anatomic landmarks on B-mode images would require a better B-mode quality and, although a fair indicator, are not sufficient to determine with certainty the exact territory perfused by a coronary artery because of the inter-individual variability of coronary anatomy (Cerqueira et al. 2002).

Left-ventricular, end-systolic radial strain is a characterization of the systolic function of the heart. However, the level of occlusion determined by invasive coronary angiography is an anatomic characterization of the severity of the stenosis. Although in animal studies it has been reported that coronary flow rate begins to fall from 50% of diameter narrowing (Gould et al. 1974), human studies have revealed a poor correlation between functional aspects, such as coronary flow rate, and myocardial perfusion and percentage of stenosis determined by coronary angiography (Gaemperli et al. 2008; Meijboom et al. 2008; Tonino et al. 2010; White et al. 1984), which is an anatomical measurement. Therefore, a stenosis superior to 50% will not always cause strain reduction. This could partially explain why radial strains did not significantly differ between the non-significant CAD and significant CAD patients. This indicates that the relationship between the severity of coronary stenosis determined by coronary angiography and the left-ventricular, end-systolic strain is complex. Geometric characteristics and composition of the plaque are additional factors of the severity of the stenosis to predict ischemia (Gaur et al. 2016). However, the results of this study are consistent with those of other studies that reported that CAD patients have lower radial (Xie et al. 2016) and longitudinal (Biering-Sorensen et al. 2014; Gaibazzi et al. 2014) strain than healthy patients.

CONCLUSIONS

Two-dimensional myocardial strain can be imaged with diverging wave imaging during a single heart cycle. Left-ventricular, end-systolic radial strains measured with myocardial elastography, at rest, were found to be higher in average in normal as compared with CAD patients. These results, if confirmed by a larger-scale study, could have a deep impact on CAD diagnosis as myocardial elastography offers promise as a screening tool for non-invasive, non-ionizing and early detection of CAD at rest.

Acknowledgments—This study was supported by the National Institutes of Health (R01-EB006042). The authors thank Rachelle Morgenstern, Joyce Moran, Tiffany Kim and Kenneth Tam for screening the patients, as well as the Nuclear Cardiology/Cardiac Stress and the Cardiac Catheterization Laboratory for their assistance.

REFERENCES

- Alam SK, Ophir J. On the use of envelope and RF signal decorrelation as tissue strain estimators. *Ultrasound Med Biol* 1997;23:1427–1433.
- Biering-Sorensen T, Hoffmann S, Mogelvang R, Zeeberg Iversen A, Galatius S, Fritz-Hansen T, Bech J, Jensen JS. Myocardial strain analysis by 2-dimensional speckle tracking echocardiography improves diagnostics of coronary artery stenosis in stable angina pectoris. *Circ Cardiovasc Imaging* 2014;7:58–65.
- Budoff M, Shinbane J. *Cardiac CT Imaging*. Berlin/New York: Springer; 2010.
- Bunting EA, Provost J, Konofagou EE. Stochastic precision analysis of 2 D cardiac strain estimation in vivo. *Phys Med Biol* 2014;59:6841–6858.
- Cerqueira MD, Weissman NJ, Dilsizian V, Jacobs AK, Kaul S, Laskey WK, Pennell DJ, Rumberger JA, Ryan T, Verani MS. Standardized myocardial segmentation and nomenclature for tomographic imaging of the heart. A statement for healthcare professionals from the Cardiac Imaging Committee of the Council on Clinical Cardiology of the American Heart Association. *Circulation* 2002;105:539–542.
- Curzen N, Rana O, Nicholas Z, Gollidge P, Zaman A, Oldroyd K, Hanratty C, Banning A, Wheatcroft S, Hobson A, Chitkara K, Hildick-Smith D, McKenzie D, Calver A, Dimitrov BD, Corbett S. Does routine pressure wire assessment influence management strategy at coronary angiography for diagnosis of chest pain? The RIPCORD study. *Circ Cardiovasc Interv* 2014;7:248–255.
- Edvardsen T, Skulstad H, Aakhus S, Urheim S, Ihlen H. Regional myocardial systolic function during acute myocardial ischemia assessed by strain Doppler echocardiography. *J Am Coll Cardiol* 2001;37:726–730.
- Gaemperli O, Schepis T, Valenta I, Koepfli P, Husmann L, Scheffel H, Leschka S, Eberli FR, Luscher TF, Alkadhi H, Kaufmann PA. Functionally relevant coronary artery disease: Comparison of 64-section CT angiography with myocardial perfusion SPECT. *Radiology* 2008;248:414–423.
- Gaibazzi N, Pigazzani F, Reverberi C, Porter TR. Rest global longitudinal 2-D strain to detect coronary artery disease in patients undergoing stress echocardiography: A comparison with wall-motion and coronary flow reserve responses. *Echo Res Pract* 2014;1:61–70.
- Gaur S, Ovrehus KA, Dey D, Leipsic J, Botker HE, Jensen JM, Narula J, Ahmadi A, Achenbach S, Ko BS, Christiansen EH, Kaltoft AK, Berman DS, Bezerra H, Lassen JF, Norgaard BL. Coronary plaque quantification and fractional flow reserve by coronary computed tomography angiography identify ischaemia-causing lesions. *Eur Heart J* 2016;37:1220–1227.
- Gould KL, Lipscomb K, Hamilton GW. Physiologic basis for assessing critical coronary stenosis: Instantaneous flow response and regional distribution during coronary hyperemia as measures of coronary flow reserve. *Am J Cardiol* 1974;33:87–94.
- Grondin J, Wan E, Gambhir A, Garan H, Konofagou E. Intracardiac myocardial elastography in canines and humans in vivo. *IEEE Trans Ultrason Ferroelectr Freq Control* 2015;62:337–349.
- Grondin J, Costet A, Bunting E, Gambhir A, Garan H, Wan E, Konofagou EE. Validation of electromechanical wave imaging in a canine model during pacing and sinus rhythm. *Heart Rhythm* 2016;13:2221–2227.
- Hoffmann S, Mogelvang R, Olsen NT, Sogaard P, Fritz-Hansen T, Bech J, Galatius S, Madsen JK, Jensen JS. Tissue Doppler echocardiography reveals distinct patterns of impaired myocardial velocities in different degrees of coronary artery disease. *Eur J Echocardiogr* 2010;11:544–549.
- Hoiland-Carsen PF, Johansen A, Christensen HW, Vach W, Moldrup M, Bartram P, Veje A, Haghfelt T. Potential impact of myocardial perfusion scintigraphy as gatekeeper for invasive examination and treatment in patients with stable angina pectoris: observational study without post-test referral bias. *Eur Heart J* 2006;27:29–34.
- Holmes JW, Borg TK, Covell JW. Structure and mechanics of healing myocardial infarcts. *Annu Rev Biomed Eng* 2005;7:223–253.
- Konofagou E, Ophir J. A new elastographic method for estimation and imaging of lateral displacements, lateral strains, corrected axial strains and Poisson's ratios in tissues. *Ultrasound Med Biol* 1998;24:1183–1199.
- Lauerma K, Virtanen KS, Sipila LM, Hekali P, Aronen HJ. Multislice MRI in assessment of myocardial perfusion in patients with single-vessel proximal left anterior descending coronary artery disease before and after revascularization. *Circulation* 1997;96:2859–2867.
- Lee WN, Ingrassia CM, Fung-Kee-Fung SD, Costa KD, Holmes JW, Konofagou EE. Theoretical quality assessment of myocardial elastography with in vivo validation. *IEEE Trans Ultrason Ferroelectr Freq Control* 2007;54:2233–2245.
- Lee WN, Qian Z, Tosti CL, Brown TR, Metaxas DN, Konofagou EE. Preliminary validation of angle-independent myocardial elastography using MR tagging in a clinical setting. *Ultrasound Med Biol* 2008;34:1980–1997.
- Lee WN, Provost J, Fujikura K, Wang J, Konofagou EE. In vivo study of myocardial elastography under graded ischemia conditions. *Phys Med Biol* 2011;56:1155–1172.
- Luo J, Konofagou EE. High-frame-rate, full-view myocardial elastography with automated contour tracking in murine left ventricles in vivo. *IEEE Trans Ultrason Ferroelectr Freq Control* 2008;55:240–248.
- Luo J, Konofagou E. A fast normalized cross-correlation calculation method for motion estimation. *IEEE Trans Ultrason Ferroelectr Freq Control* 2010;57:1347–1357.
- Luo J, Bai J, He P, Ying K. Axial strain calculation using a low-pass digital differentiator in ultrasound elastography. *IEEE Trans Ultrason Ferroelectr Freq Control* 2004;51:1119–1127.
- Ma C, Varghese T. Comparison of cardiac displacement and strain imaging using ultrasound radiofrequency and envelope signals. *Ultrasonics* 2013;53:782–792.
- Meijboom WB, Van Mieghem CA, van Pelt N, Weustink A, Pugliese F, Mollet NR, Boersma E, Regar E, van Geuns RJ, de Jaegere PJ, Serruys PW, Krestin GP, de Feyter PJ. Comprehensive assessment of coronary artery stenoses: Computed tomography coronary angiography versus conventional coronary angiography and correlation with fractional flow reserve in patients with stable angina. *J Am Coll Cardiol* 2008;52:636–643.
- Montalescot G, Sechtem U, Achenbach S, Andreotti F, Arden C, Budaj A, Bugiardini R, Crea F, Cuisset T, Di Mario C, Ferreira JR, Gersh BJ, Gitt AK, Hulot JS, Marx N, Opie LH, Pfisterer M, Prescott E, Ruschitzka F, Sabate M, Senior R, Taggart DP, van der Wall EE, Vrints CJ, Zamorano JL, Baumgartner H, Bax JJ, Bueno H, Dean V, Deaton C, Erol C, Fagard R, Ferrari R, Hasdai D, Hoes AW, Kirchhof P, Knutti J, Kolh P, Lancellotti P, Linhart A, Nihoyannopoulos P, Piepoli MF, Ponikowski P, Sirtes PA, Tamargo JL, Tendera M, Torbicki A, Wijns W, Windecker S, Valgimigli M, Claeys MJ, Donner-Banzhoff N, Frank H, Funck-Brentano C, Gaemperli O, Gonzalez-Juanatey JR, HAMILTON, Husted S, James SK, Kervinen K, Kristensen SD, Maggioni AP, Pries AR, Romeo F, Ryden L, Simoons-Sel A, Steg PG, Timmis A, Yildirim A. 2013 ESC guidelines on the management of stable coronary artery disease: The Task Force on the management of stable coronary artery disease of the European Society of Cardiology. *Eur Heart J* 2013;34:2949–3003.
- Mozaffarian D, Benjamin EJ, Go AS, Arnett DK, Blaha MJ, Cushman M, de Ferranti S, Despres JP, Fullerton HJ, Howard VJ, Huffman MD, Judd SE, Kissela BM, Lackland DT, Lichtman JH, Lisabeth LD, Liu S, Mackey RH, Matchar DB, McGuire DK, Mohler ER III, Moy CS, Muntner P, Mussolino ME, Nasir K, Neumar RW, Nichol G, Palaniappan L, Pandey DK, Reeves MJ, Rodriguez CJ, Sorlie PD, Stein J, Towfighi A, Turan TN, Virani SS, Willey JZ, Woo D, Yeh RW, Turner MB. Heart disease

- and stroke statistics—2015 update: A report from the American Heart Association. *Circulation* 2015;131:e29–e322.
- Papadacci C, Pernot M, Couade M, Fink M, Tanter M. High-contrast ultrafast imaging of the heart. *IEEE Trans Ultrason Ferroelectr Freq Control* 2014;61:288–301.
- Park HB, Heo R, o Hartaigh B, Cho I, Gransar H, Nakazato R, Leipsic J, Mancini GB, Koo BK, Otake H, Budoff MJ, Berman DS, Erglis A, Chang HJ, Min JK. Atherosclerotic plaque characteristics by CT angiography identify coronary lesions that cause ischemia: A direct comparison to fractional flow reserve. *JACC Cardiovasc Imaging* 2015;8:1–10.
- Patel MR, Peterson ED, Dai D, Brennan JM, Redberg RF, Anderson HV, Brindis RG, Douglas PS. Low diagnostic yield of elective coronary angiography. *N Engl J Med* 2010;362:886–895.
- Provost J, Gambhir A, Vest J, Garan H, Konofagou EE. A clinical feasibility study of atrial and ventricular electromechanical wave imaging. *Heart Rhythm* 2013;10:856–862.
- Provost J, Nguyen VT, Legrand D, Okrasinski S, Costet A, Gambhir A, Garan H, Konofagou EE. Electromechanical wave imaging for arrhythmias. *Phys Med Biol* 2011;56:L1–L11.
- Roth GA, Forouzanfar MH, Moran AE, Barber R, Nguyen G, Feigin VL, Naghavi M, Mensah GA, Murray CJ. Demographic and epidemiologic drivers of global cardiovascular mortality. *N Engl J Med* 2015;372:1333–1341.
- Schuijf JD, Wijns W, Jukema JW, Atsma DE, de Roos A, Lamb HJ, Stokkel MP, Dibbets-Schneider P, Decramer I, De Bondt P, van der Wall EE, Vanhoenacker PK, Bax JJ. Relationship between noninvasive coronary angiography with multi-slice computed tomography and myocardial perfusion imaging. *J Am Coll Cardiol* 2006;48:2508–2514.
- Shaw LJ, Hachamovitch R, Berman DS, Marwick TH, Lauer MS, Heller GV, Iskandrian AE, Kesler KL, Travin MI, Lewin HC, Hendel RC, Borges-Neto S, Miller DD. The economic consequences of available diagnostic and prognostic strategies for the evaluation of stable angina patients: an observational assessment of the value of precatheterization ischemia. *Economics of Noninvasive Diagnosis (END) Multicenter Study Group. J Am Coll Cardiol* 1999;33:661–669.
- Svealy BG, Olofsson EL, Andersson B. Ventricular long-axis function is of major importance for long-term survival in patients with heart failure. *Heart* 2008;94:284–289.
- Tonino PA, Fearon WF, De Bruyne B, Oldroyd KG, Leesar MA, Ver Lee PN, Maccarthy PA, Van't Veer M, Pijls NH. Angiographic versus functional severity of coronary artery stenoses in the FAME study fractional flow reserve versus angiography in multivessel evaluation. *J Am Coll Cardiol* 2010;55:2816–2821.
- Urheim S, Edvardsen T, Torp H, Angelsen B, Smiseth OA. Myocardial strain by Doppler echocardiography. Validation of a new method to quantify regional myocardial function. *Circulation* 2000;102:1158–1164.
- Vasan RS, Larson MG, Benjamin EJ, Evans JC, Reiss CK, Levy D. Congestive heart failure in subjects with normal versus reduced left ventricular ejection fraction: Prevalence and mortality in a population-based cohort. *J Am Coll Cardiol* 1999;33:1948–1955.
- Voigt JU, Exner B, Schmiedehausen K, Huchzermeyer C, Reulbach U, Nixdorff U, Platsch G, Kuwert T, Daniel WG, Flachskampf FA. Strain-rate imaging during dobutamine stress echocardiography provides objective evidence of inducible ischemia. *Circulation* 2003;107:2120–2126.
- Weidemann F, Jung P, Hoyer C, Broscheit J, Voelker W, Ertl G, Stork S, Angermann CE, Strotmann JM. Assessment of the contractile reserve in patients with intermediate coronary lesions: A strain rate imaging study validated by invasive myocardial fractional flow reserve. *Eur Heart J* 2007;28:1425–1432.
- White CW, Wright CB, Doty DB, Hiratza LF, Eastham CL, Harrison DG, Marcus ML. Does visual interpretation of the coronary arteriogram predict the physiologic importance of a coronary stenosis? *N Engl J Med* 1984;310:819–824.
- Winter R, Jussila R, Nowak J, Brodin LA. Speckle tracking echocardiography is a sensitive tool for the detection of myocardial ischemia: A pilot study from the catheterization laboratory during percutaneous coronary intervention. *J Am Soc Echocardiogr* 2007;20:974–981.
- Xie MY, Lv Q, Wang J, Yin JB. Assessment of myocardial segmental function with coronary artery stenosis in multi-vessel coronary disease patients with normal wall motion. *Eur Rev Med Pharmacol Sci* 2016;20:1582–1589.
- Zervantonakis IK, Fung-Kee-Fung SD, Lee WN, Konofagou EE. A novel, view-independent method for strain mapping in myocardial elastography: Eliminating angle and centroid dependence. *Phys Med Biol* 2007;52:4063–4080.
- Zuo H, Yan J, Zeng H, Li W, Li P, Liu Z, Cui G, Lv J, Wang D, Wang H. Diagnostic power of longitudinal strain at rest for the detection of obstructive coronary artery disease in patients with type 2 diabetes mellitus. *Ultrasound Med Biol* 2015;41:89–98.